Green Chemistry

PAPER

View Article Online
View Journal | View Issue

Cite this: *Green Chem.*, 2021, **23**, 1361

Sequential acid-catalyzed alkyl glycosylation and oligomerization of unprotected carbohydrates†

Lea Spitzer, [a,b] Sébastien Lecommandoux,[b] Henri Cramail*[b] and François Jérôme *[a]

Received 11th December 2020,
Accepted 15th January 2021

DOI: 10.1039/d0gc04198j

rsc.li/greenchem

An efficient method has been developed to synthesize end-functionalized oligosaccharides from unprotected monosaccharides in a one-pot/two-step approach. In the first step, mannose (and glucose) was functionalized with an alkyne group at the anomeric position through the Fisher-glycosylation reaction with propargyl alcohol as a glycosyl acceptor. In the second step, the functionalized monosaccharides were oligomerized and the experimental conditions were optimized by varying the temperature, time and the molar ratio between alcohol and sugar to reach a $\overline{DP_n}$ up to 8. The obtained oligosaccharides showed complete propargylation at their reducing chain-end and were successfully coupled to oleic acid *via* the Huisgen reaction, affording bio-based surfactants.

Introduction

Surfactants are ubiquitous molecules in our daily life with multiple applications in various sectors such as home and personal care, paint, food, medicine, water treatment, materials, *etc*.[1–3] Due to the exponential increase of the world population, and also due to several emerging economies worldwide, our society's demand for surfactants is increasing dramatically. This market, of about 12 million tons per year, is expected to grow at an annual rate of 4.3%.[4] Because of environmental concerns, the manufacture of bio-based surfactants has become increasingly attractive, as it potentially provides more environmentally friendly products, although a full life cycle assessment should be systematically carried out to support this claim.[3,5–9] The market of bio-based surfactants[10] is about 3.5 million tons per year in Europe, a region where the annual growth rate of bio-based surfactants was 3% between 2008 and 2013, with alkylpolyglycosides (APGs) registering the strongest growth.[11–14]

APGs are industrially produced through the acid-catalyzed Fischer glycosylation reaction.[14–17] This reaction couples unprotected monomeric sugars with long chain alkyl alcohols (C_5–C_{18}) and releases a stoichiometric amount of water. During the Fisher glycosylation, the *in situ* produced monomeric alkyl glycosides tend to further react with unconverted sugars, leading to the formation of APGs. Due to the release of water, concomitant oligomerization of the sugar head and hydrolysis of the glycosidic bond occur, leading to a thermodynamic equilibrium in which APGs are composed, on average, of 1.5 to 2.1 sugar units per fatty chain. Being able to increase the degree of polymerization ($\overline{DP_n}$) of sugar units per fatty chain is of great interest, as it modifies the hydrophilic–lipophilic balance (HLB) of APGs, and consequently their performances. For instance, this can tune their physicochemical properties in terms of water solubility, foaming properties, critical micelle concentrations, surface tensions, *etc*. However, this elongation of the sugar moiety remains a very challenging task. The main hurdle is the *in situ* release of water, which induces a rapid hydrolysis of glycosidic bonds, even when water is continuously distilled out. Furthermore, at the end of the reaction, the removal of the excess of fatty alcohols by distillation is a very delicate step as it generally requires elevated temperatures, leading to the partial degradation of APGs. So far, all attempts to produce APGs with a $\overline{DP_n}$ larger than 2.1 have failed. One should mention that enzymatic catalysis potentially paves the way to APGs with a larger $\overline{DP_n}$, but the cost of the enzymes and the low reactor productivity hamper the implementation of these routes on a bigger scale.[18–21]

In this work, we propose an alternative straightforward strategy based on the use of propargyl alcohol (PGA), which serves not only as a glycosyl acceptor but also as a linker to subsequently introduce the fatty chain through a 100% atom-economical copper-catalyzed Huisgen reaction. In contrast to fatty alcohols, at the end of the reaction, PGA can be conveniently separated by distillation at a low temperature, limiting the degradation of APGs. Importantly, as sugars are more

[a]*INCREASE/Institut de Chimie des Milieux et Matériaux de Poitiers, CNRS, Université de Poitiers, 1 rue Marcel Doré, 86073 Poitiers cedex 9, France. E-mail: francois.jerome@univ-poitiers.fr*
[b]*INCREASE/Université de Bordeaux, CNRS, Bordeaux INP, LCPO, UMR 5629, F-33600 Pessac, France*

†Electronic supplementary information (ESI) available: NMR, GC-FID, ESI-MS and MALDI-TOF spectra. See DOI: 10.1039/d0gc04198j

soluble in PGA than in fatty alcohols, oligomerization takes place to a larger extent during the evaporation step of PGA, leading to the formation of APGs with a $\overline{DP_n}$ of 8.

Experimental

Chemicals

D-(+)-Mannose (from wood, ≥99%), D-(+)-glucose (≥99.5%) and Amberlyst-15 (≥90%, 0.355–1.18 mm, 1.7 ml L^{-1} capacity) were purchased from Sigma Aldrich, and dried under vacuum before use. GC-FID standards propargyl α-D-mannopyranoside (PMan) and 1,6-anhydro-β-D-mannopyranose (AMP) were purchased from Biosynth Carbosynth. Propargyl alcohol (99%), BSTFA (+1% TMCS), D-sorbitol (≥98%), 1,5,7-triazabicyclo [4.4.0]dec-5-ene (98%, TBD), sodium azide (reagent plus ≥99.5%), L-ascorbic acid (99%) and 3-bromo-1-propanol (97%) were purchased from Sigma Aldrich and used without further purification. Methyl oleate (MeOI ≥ 99.9%) was obtained from Nuchekrep. Cuprisorb was purchased from Seachem and copper(II) sulfate from ProLabo. Acetone, acetonitrile, chloroform ($CDCl_3$), diethyl ether, dimethyl sulfoxide (DMSO), ethyl acetate (EtOAc), petroleum ether (PE), pyridine and magnesium sulfate were purchased from Sigma Aldrich and used without further purification. Dialysis was performed using a Spectra/Por®6 MWCO 100–500 Da membrane (RC).

Synthesis procedure

General method of the Fischer glycosylation and oligomerization of mannose. - *Step 1* -

In a round-bottom flask, mannose (5 g, 27.75 mmol) was dispersed in an excess of propargyl alcohol (5 eq.) and stirred at 80 °C in the presence of amberlyst-15 (4.2 mol% H^+) for 3 h. Then, the reaction was stopped, and the as-obtained yellow/orange solution was separated by centrifugation from the catalyst. The as-recovered solution (pH 4) was used for the following step without further purification.

- *Step 2* -

Oligomerization was attained by removing the excess of propargyl alcohol through heating of the mixture of step 1 at 100 °C for 4 h under vacuum. Note that for analysis only, the trace amount of free propargyl alcohol was fully removed as follows: $(PMan)_n$ was dissolved in water, and a trace of propargyl alcohol was extracted with chloroform. The aqueous phase was then freeze-dried to give a brown-beige solid (4.3 g, 88%). It could be additionally purified by filtration over active carbon, yielding a white powder (**S1**). $Đ$ (SEC) = 2.03; ATR-IR = 2116 (C≡C str.) (s); ^{1}H-NMR (400 MHz, D_2O): δ = 5.32–5.08 (m, 1.66 H), 5.08–5.01 (d_b, 2 H), 4.97–4.90 (db, 3.23 H), 4.73 (d, 0.44 H), 4.41–4.32 (m, 6.56 H, CH_2), 4.15–3.53 (m, 49.86 H, α/β-H2–α/β-H-6), 3.42–3.39 (tq, 0.74 H, β-H-5), 2.95 (t_b, 1 H, alkyne); ^{13}C-NMR (100.4 MHz, D_2O): δ = 102.4, 102.3, 100.5, 99.5, 99.2, 99.0, 98.6, 97.0, 78.7, 78.3, 78.1, 76.2, 73.2, 72.9, 72.7, 71.3, 70.6, 70.5, 70.3, 69.9, 69.8, 66.7, 66.4, 65.4, 60.9, 54.7, 54.6.

Characterization methods

Nuclear magnetic resonance (NMR). NMR spectra were obtained on a Bruker Advance III 400. Typically, 10–20 mg of the sample was diluted in 0.5 mL of deuterated solvent before the measurement. The following reference values of deuterated solvents were used: D_2O (^{1}H-NMR: δ = 4.8 ppm). The spectral data were analyzed using TopSpin (v. 4.0.9). Automatic phase correction and subsequent integration were applied.

Matrix assisted laser desorption/ionisation-time of flight (MALDI-TOF). MALDI-MS spectra were recorded by CESAMO (Bordeaux, France) on an Autoflex maX TOF mass spectrometer (Bruker Daltonics, Bremen, Germany) equipped with a frequency tripled Nd:YAG laser emitting at 355 nm. Spectra were recorded in the positive-ion linear mode and with an accelerating voltage of 19 kV. The samples were dissolved at 20 mg mL^{-1} (water : acetonitrile 70/30 + trifluoroacetic acid (TFA, 10 vol%). A 2,5-dihydroxybenzoic acid (DHB) matrix solution was prepared by dissolving 10 mg in 1 mL of acetonitrile. The solutions were combined in 10 : 1 v/v of matrix to sample. One to two microliters of the obtained solution were deposited onto the sample target and vacuum-dried.

Size exclusion chromatography (SEC). Polymer molar masses were determined by Size Exclusion Chromatography (SEC) using water as the eluent. Measurements in water were performed on an Ultimate 3000 system from Thermoscientific equipped with a diode array detector (DAD). The system also includes a multi-angle laser light scattering detector MALLS and a differential refractive index detector dRI from Wyatt technology. Polymers were separated on two Shodex OH Pack 802.5 (8 × 300) columns (exclusion limits from 500 Da to 10 000 Da) at a flow rate of 0.6 mL min^{-1}. The column temperature was held at 25 °C. Dextran from PSS was used as the standard.

Attenuated total reflectance infrared spectroscopy (ATR-IR). Fourier transform infrared (FTIR) spectra were recorded on a Bruker VERTEX 70 instrument (4 cm^{-1} resolution, 64 scans, DLaTGS MIR) equipped with a Pike GladiATR plate (diamond crystal) for attenuated total reflectance (ATR) analysis at room temperature.

Gas chromatography with flame-ionization detection (GC-FID). The composition of the mono- and disaccharide fractions was analyzed by GC-FID spectroscopy after the transformation of the sugar components into their corresponding per-*O*-trimethylsilyl (nonreducing sugars) or per-*O*-trimethylsilylated oxime (reducing sugars). The crude samples (in general 20–30 mg) were dissolved in 1 mL of pyridine (containing 1 mg mL^{-1} sorbitol as an internal standard). To 100 μL of the resulting solution was then added 200 μL of BSTFA (+1% TMCS), and the mixture was stirred at RT for 2 h. During this operation, a white precipitate was observed, which was separated by filtration (0.45 μm, regenerated cellulose) before injection into the apparatus.[22] By this procedure, the non-reducing sugars gave single peaks in the chromatogram, whereas the reducing sugars afforded two peaks for the corresponding *syn* and *anti* TMS-oximes. The identification and quantification were achieved by comparison with authentic standards for

which the response factors were obtained from the corresponding calibration curves using sorbitol as the internal standard. The analysis was conducted with a GC Trace 1300 Gas Chromatograph (Thermoscientific) equipped with a split/splitness injector and flame ionization detector (FID). A H_2 flow rate of 34 mL min^{-1} and an airflow rate of 350 mL min^{-1} were used. The flow rate of the carrier gas (H_2) was set at 1.2 mL min^{-1}. The temperatures of the injection port and detector were set at 250 °C and 320 °C, respectively. The oven temperature was programmed to initiate at 90 °C for 1 min, and then the temperature was raised to 220 °C at a rate of 10 °C min^{-1} and finally increased to 320 °C at a rate of 40 °C min^{-1} and held there for 5 min. The injection volume was 1 μL in the split injection mode (15 : 1). Separation was performed on a capillary column TRB-5MS (30 m × 0.25 mm × 0.25 mm film thickness) from Teknokroma with matrix 95% dimethyl-(5%) diphenyl polysiloxane.

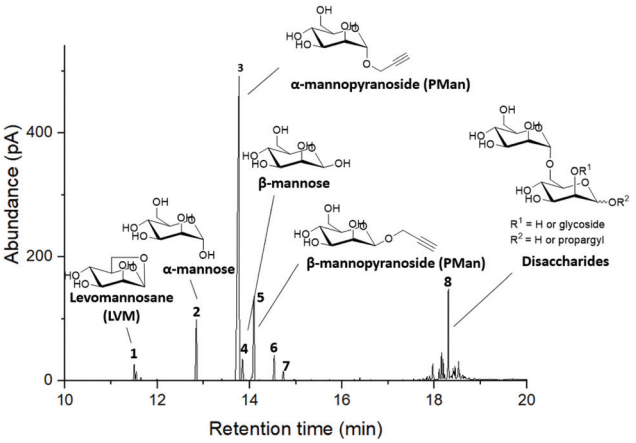

Fig. 1 Typical GC-FID spectrum collected after step 1.

Results and discussion

The present study should be viewed as a two-step process in which step 1 is the acid-catalyzed glycosylation of monomeric sugars with PGA, and step 2 is the elongation of the sugar moiety (Scheme 1). As a case study, mannose was first selected. Transposition to glucose is discussed in the second part.

Step 1. Glycosylation of mannose with PGA

In the first set of experiments, unprotected mannose was suspended in a 5-fold excess of PGA, the latter serving as both a glycosyl acceptor and solvent. The resulting mixture was stirred at 80 °C in the presence of Amberlyst-15, a solid acid catalyst (4.2 mol% of H^+). The reaction was monitored by gas chromatography (GC) over a period of 48 h. A sequential oximation–trimethylsilylation derivatization procedure was used to calculate the conversion of mannose and to quantify the mono- and disaccharide fractions.

After 48 h (Fig. 1), GC clearly revealed a conversion of mannose (α-mannose, peak **2**, β-mannose, peak **4**) of 93%, accompanied by the formation of α/β propargyl-(mono)-mannopyranoside in 69% yield (PMan, peak **3** and **5**). Other detected products were disaccharides (peak **8**), levomannosane (LVM, peak **1**) and also minor products (such as furanoside peak **6** and acyclic acetal peak 7), in a relative proportion of 20%, 3% and 8%, respectively. The retention times of standard chemicals are given in Fig. S2 and Table S1.† By means of size exclusion chromatography, propargyl-(oligo)-mannosides $(PMan)_n$ were also detected (Fig. S3†). In line with previous reports, the $\overline{DP_n}$ of $(PMan)_n$, determined by ^{1}H-NMR (see later for more information) was 1.3, showing that oligomerization occurs to a very low extent under these conditions.

A plot of the PMan yields as a function of reaction time is provided in Fig. 2. It shows that the PMan yield and the mannose conversion levelled off around 70% and 90%, respectively, after 7 h of reaction. Extending the reaction time from 7 to 48 h did not result in the complete conversion of mannose, suggesting that the system has reached a thermodynamic equilibrium.

We next studied the influence of temperature (Fig. 3). Decreasing the reaction temperature from 100 °C to 80 °C

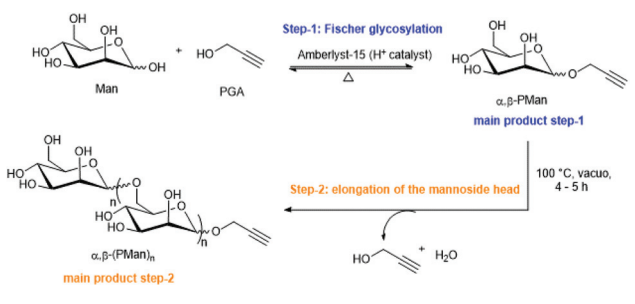

Scheme 1 Summarized method of the preparation of $(PMan)_n$ through 2 steps: step 1 = mannose (1 eq.) + PGA (5 eq.) + Amberlyst-15 (4.2 mol%), 80 °C, 1–12 h; step 2 = vacuum at 100 °C for 4–5 h. For the sake of clarity, only the pyranoside form is represented.

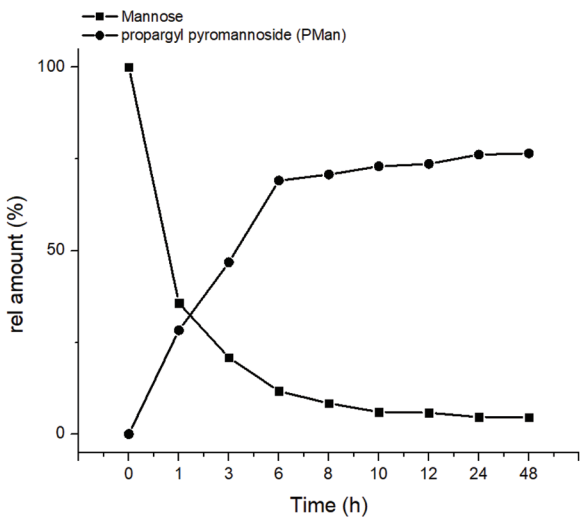

Fig. 2 Mannose conversion and PMan yield as a function of reaction time (80 °C, PGA/mannose molar ratio = 5, Amberlyst-15 (4.2 mol% H^+)).

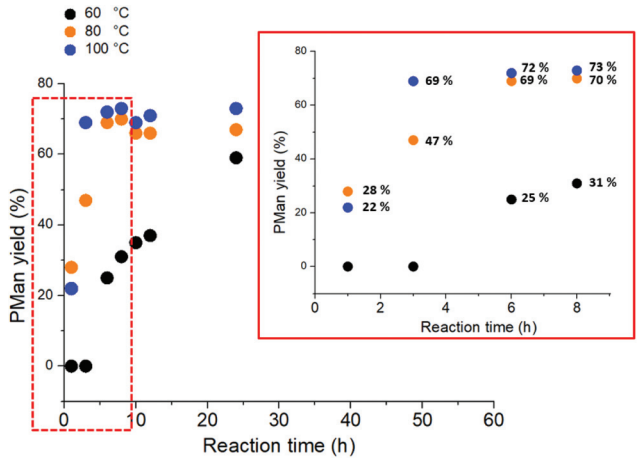

Fig. 3 Effect of the reaction temperature on the PMan formation rate (PGA/mannose molar ratio = 5, Amberlyst-15 (4.2 mol% H^+)).

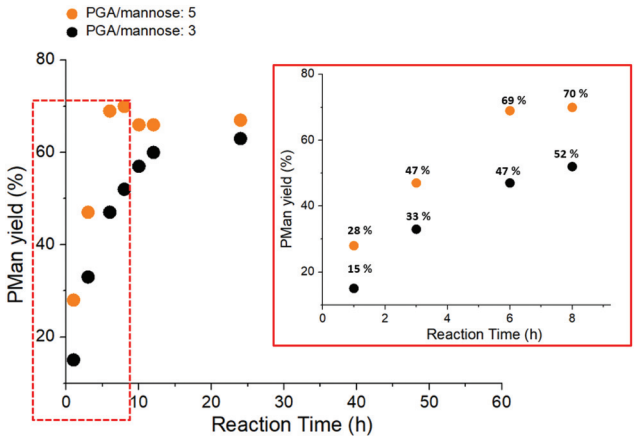

Fig. 4 Effect of the PGA/mannose molar ratio on the PMan formation rate (80 °C, Amberlyst-15 (4.2 mol% H^+)).

obviously decreased the reaction rate (from 23 mol h^{-1} to 9.5 mol h^{-1}). For instance, after 3 h of reaction, 90% and 79% of mannose were converted at 100 °C and 80 °C, respectively. When lowering the temperature further to 60 °C, we faced problems of immiscibility between mannose and PGA.

However, at 60 °C, the reaction started after 6 h, and a conversion of mannose of about 80% was observed after 12 h of reaction (2.5 mol h^{-1}). This 6 h induction period corresponds to the time to completely dissolve mannose in PGA at 60 °C.

Seeking for a compromise between the stability of mannose and the reaction rate, the reaction temperature was fixed at 80 °C in the following experiments. Note that decreasing the PGA/mannose molar ratio from 5 to 3 slowed down the reaction rate from 6.2 mol h^{-1} to 4.5 mol h^{-1}, tentatively attributed to an increase of the reaction medium viscosity. However, this did not significantly impact either the PMan yield (Fig. 4) or the $\overline{DP_n}$ of $(PMan)_n$ recovered in step 1, confirming that the *in situ* released water prevents oligomerization to a large extent.

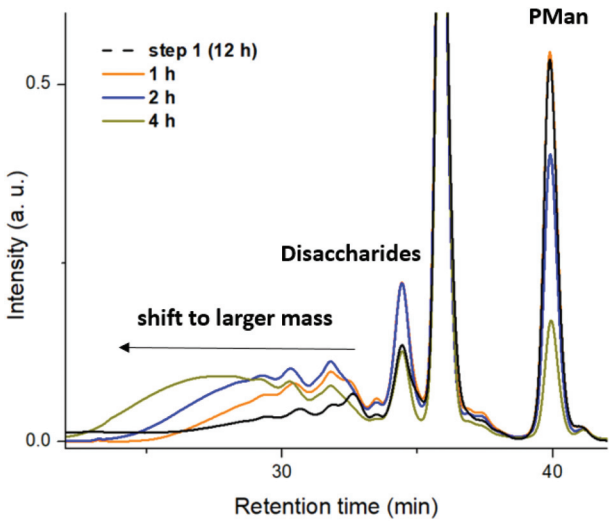

Fig. 5 Overlaid SEC (measured against dextran-standards in H_2O at 25 °C) spectra during step 2 (100 °C, vacuum).

Step 2. Oligomerization of the sugar head

In order to increase the $\overline{DP_n}$ of PMan, the reaction mixture was then heated under vacuum at 100 °C to distill out the excess of PGA and the *in situ* released water. The time needed to evaporate the excess of PGA (4 h) restricted the duration of the reaction. The effect of this treatment on the average $\overline{DP_n}$ was monitored by SEC. As shown in Fig. 5, after 4 h under vacuum, a shift towards high molar masses was clearly observed, a result consistent with the elongation of the sugar moiety. This treatment was accompanied by the formation of a beige-brownish powder. After complete removal of PGA, only 5–8% of monomeric species remained (determined by gas chromatography). The molar mass of the total batch was 1353 g mol^{-1} (*i.e.*, $\overline{DP_n} = 8$) with a dispersity, $Đ$, of around 2.

Note that distilled PGA can be reused for further glycosylation reactions in step 1, but only after drying over magnesium sulfate to remove traces of water.

To get more information on the structures of the oligomers formed, NMR investigations were performed (Fig. 6). Owing to the low field shift of the alkyne proton (2.95 ppm), the end-group method could be employed to calculate the degree of oligomerization, and indirectly the average molar mass. The $\overline{DP_n}$ and $\overline{M_n}$ values were calculated from the ^{1}H-NMR spectra using the following equations:

$$\overline{DP_n} = \frac{(H2 + H3 + H4 + H5 + H6)}{6} \quad (1)$$

$$\overline{M_n} = 179 + M_0 DP_n + 201 \quad (2)$$

where M_0 is the repeating unit with a molar mass of 162 g mol^{-1}. The values of 179 g mol^{-1} and 201 g mol^{-1} are derived from the end groups of $(PMan)_n$ (Fig. S4†). A detailed analysis by one- and two-dimensional NMR spectroscopy, including the $^nJ_{H-H}$ and $^nJ_{C-H}$ couplings, is given in the ESI (Fig. S5–S7†).

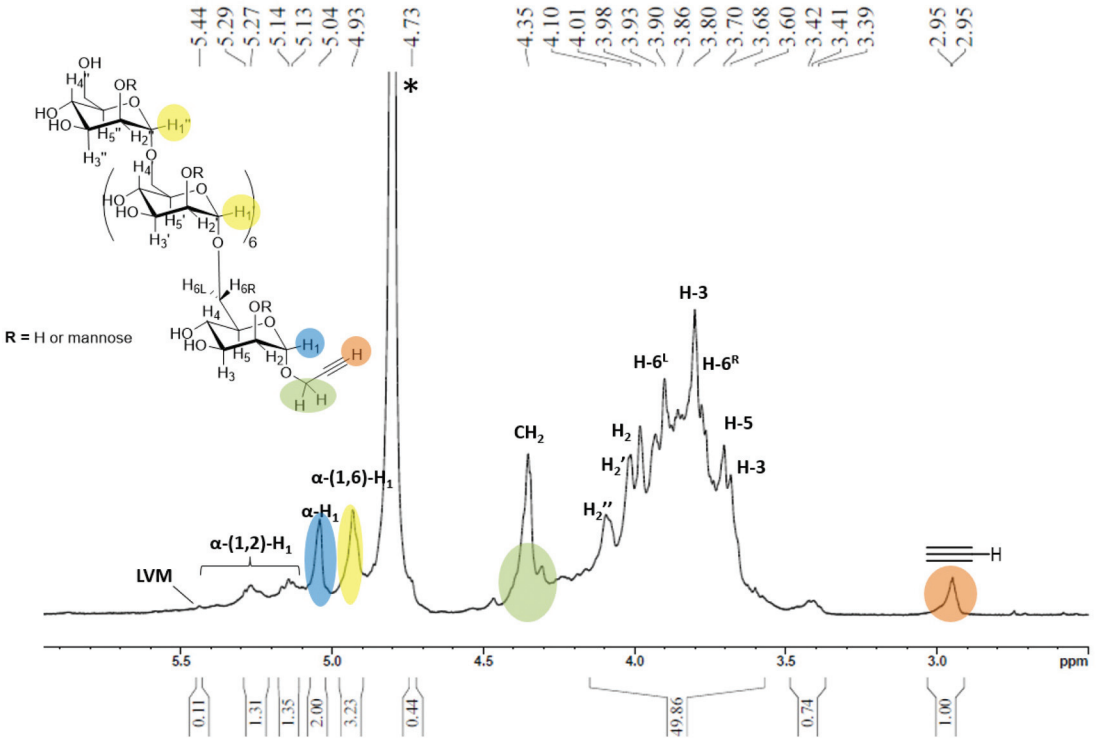

Fig. 6 ^{1}H-NMR (400 MHz, D_2O) spectrum of $(PMan)_n$; $\overline{DP_n} = 8$, $\overline{M_n} = 1353\ g\ mol^{-1}$.

The signals at 2.95 ppm (brown, HC≡) and 4.32–4.41 ppm (green, CH_2) confirmed the coupling of oligomannosides with PGA (Fig. 6). Indeed, these signals chemically shifted downfield as compared to pure PGA (2.80 ppm (HC≡) and 4.20 ppm (CH_2)). The broad peak at 5.01–5.08 ppm was assigned to the anomeric proton (blue, α-H-1) located in the α position at the chain end of $(PMan)_n$. The assignment of this proton could be further confirmed either with the reference signal of pure monomeric PMan at 5.06–5.05 ppm (Fig. S8†)[23,24] or with a coupling constant of 4 Hz between α-H-1 and the –CH_2– of PGA in the NMR HMBC spectrum (Fig. S7†). The spectrum in Fig. 6 showed additional peaks in the range of 4.90 to 5.32 ppm. This region is characteristic of the anomeric protons and was thus attributed to the glycosidic linkages between the anhydromannose units in the oligomannoside chain. The most intense peak at 4.93 ppm (yellow in Fig. 6) was assigned to the anomeric proton of the α-(1,6)-glycosidic linkage. This claim is supported by NMR NOESY experiments (Fig. S6†) showing a proton–proton long range coupling of this anomeric proton with the H-6 protons of the anhydromanose unit. The α configuration was also supported by the HMBC spectrum with a carbon–proton coupling of 171.32 Hz (Fig. S7†).[25] The additional multiplet signals appearing between 5.08 and 5.32 ppm were tentatively attributed to the α-(1,2)-glycosidic linkages, as COSY- and NOESY NMR spectroscopy (Fig. S5 and S6†) showed an exclusive H,H-coupling with H-2 protons of the mannose ring (4.1–3.98 ppm). On the basis of the signal intensity, the oligomannoside chain is dominantly assembled through α-(1,6)-glycosidic bonds and, to a lower extent, through α-(1,2)-glycosidic linkages (Fig. S9 and Table S2†). One should note that the additional peak at 4.73 ppm suggests the existence of β-glycosidic linkages. This was supported by the proton–proton long range coupling to β-H-5 (3.41 ppm) in the NMR NOESY spectrum (Fig. S6†). However, due to the poor intensity in the 2D-NMR spectra, they were present in very low percentages. Integration of the different anomeric signals in the ^{1}H NMR spectrum (Fig. 6) suggested that the oligomannoside chain is composed of 60% of α-(1,6)-linkages, 24% of α-(1,2)-linkages, and only 8% of β-(1,6) and β-(1,2) linkages. Another small doublet found at 5.44 ppm accounted for 5% relative to all anomeric protons and was assigned to the anomeric proton of levomannosane (LVM). This chemical composition is also supported by ^{13}C NMR (Fig. S10†). This structure is actually very similar to what was previously observed in the oligomerization of mannose by high frequency ultrasound,[26] the 1–6 linkages being thermodynamically the most favorable ones.

To further support this chemical composition, the samples were analyzed by MALDI-TOF spectrometry (Fig. 7). The data showed a series of monoanionized peaks with sequential increments of m/z = 162 Da (corresponding to the anhydromannose residue as the repeating unit). This series was assigned to $(PMan)_n$, and DP up to 12 was detected, which corresponds to a $\overline{DP_n}$ of 8 as calculated by NMR (eqn (1)). Within the noise of the MS spectra, a second series, with m/z lower than 56 as compared to $(PMan)_n$, was observed and corresponded to the formation of an oligomannoside terminated by a dehydrated anydromannose residue. The formation of

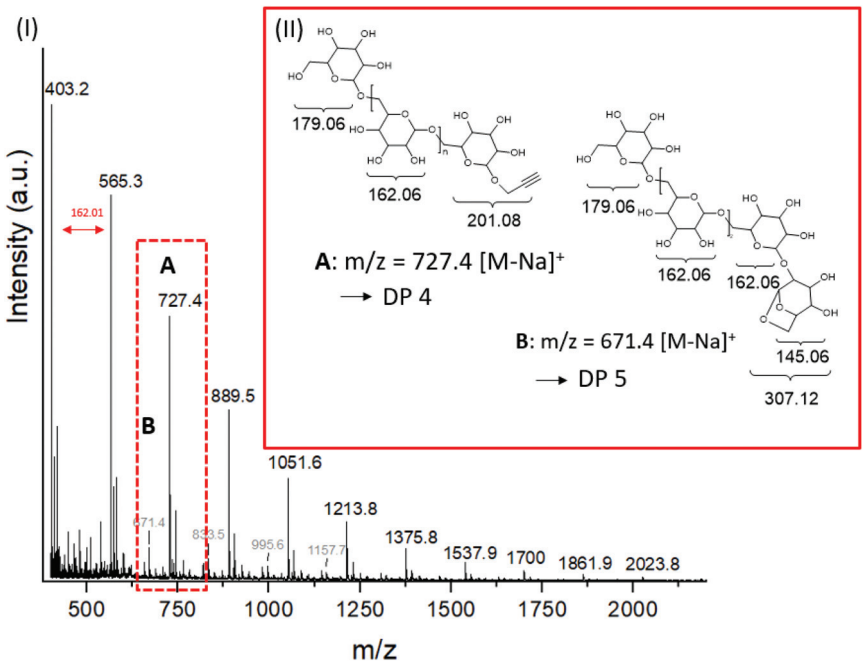

Fig. 7 (I) MALDI-TOF spectrum of $(PMan)_n$ recovered after step 2; (II) proposed structures.

this oligomannoside series remained however quasi negligible, as also supported by NMR investigations. This combined NMR-mass analysis led us to conclude that the as-obtained oligomannosides are (1) fully propargylated at their terminal end, (2) mainly linked through α-(1,6)-linkages and (3) exhibit a $\overline{DP_n}$ up to 8. By means of DSC analysis, the T_g of $(PMan)_8$ was found to be 120 °C.

To further increase the $\overline{DP_n}$ of $(PMan)_n$, step 1 was stopped before the complete conversion of mannose; this should facilitate the reaction of PMan with the unreacted mannose in step 2. When the glycosylation of mannose with PGA was stopped after 1–3 h at 80 °C in step 1, 21–36% of free mannose remained unreacted. When vacuum (step 2) was applied at that stage, the unreacted free mannose randomly polymerized either with PMan or other molecule of mannose. Unfortunately, a mixture of $(PMan)_n$ (76%) and terminal free oligomannoside (12%) along with 12% of LVM was obtained. To ensure the elongation of the sugar moiety and full glycosylation with PGA at the terminal position, it is thus mandatory to achieve a nearly complete conversion of mannose in step 1 prior to step 2, suggesting also that step 1 is reversible under vacuum (see later for more information). The best conditions in step 1 are 80 °C, a PGA/mannose molar ratio of 5, and 3 h of reaction, leading to the formation of PMan in 65% yield (step 1) and $(PMan)_n$ with a $\overline{DP_n}$ of 8 in step 2 (Fig. 6).

Plausible reaction mechanism

On the basis of all these results, we suggest a plausible reaction mechanism (Scheme 2), inspired by the most accepted proposals of glycosylation in the literature.[27–29] In step 1, mannose is protonated by amberlyst-15 to form the oxocarbenium ion, which is then rapidly trapped by PGA to form PMan. The elongation of the mannose moiety to form APGs occurs to a very low extent in step 1, mainly due to the excess of PGA and the *in situ* release of water which prevents the oligomerization reaction. In step 2, PMan is reprotonated, partly regenerating the oxocarbenium ion, as previously suggested by Mamidyala *et al.*[30] During the distillation of PGA (and water) under vacuum, the reaction of the oxocarbenium ion with PMan is statistically more likely to occur, leading to the formation of $(PMan)_n$ with a $\overline{DP_n}$ of 8. To confirm the mechanism of step 2, PMan was prepared, isolated by chromatography over silica gel (acetonitrile/water (10–30 vol%)) and freeze dried for at least two days. Then, purified PMan was dissolved in PGA (5 equiv.) and stirred at 80 °C for 1 h (step 1) with Amberlyst-15 prior to heating the mixture at 100 °C under vacuum for 4 h (step 2). Under these conditions, PMan was converted to $(PMan)_n$ with a $\overline{DP_n}$ of 4, in 85% yield (Fig. S11†). These findings support that PMan could be depropargylated to form the oxocarbenium ion back, which can further react with another species of PMan, resulting in the elongation of the mannoside chain. One should note that this oligomerization reaction is possible, thanks to the solubility of mannose and APGs in PGA. In contrast, with fatty alcohols, this elongation was not observed in step 2 due to the solubility issue, *i.e.*, the precipitation (and/or degradation) of monoalkylglycosides and sugars upon evaporation. The proposed reaction mechanism also explains the formation of LVM as a minor product, resulting from the internal cyclization of the oxocarbenium ion.

Note that Amberlyst-15 can be replaced by strongly acidic H_2SO_4 or Aquivion PFSA. However, due to the high acid strength of these acids, the proton loading has to be reduced from 4.2 mol% to 0.13 mol% to avoid fast and uncontrolled degradation of sugars, in particular in step 2.

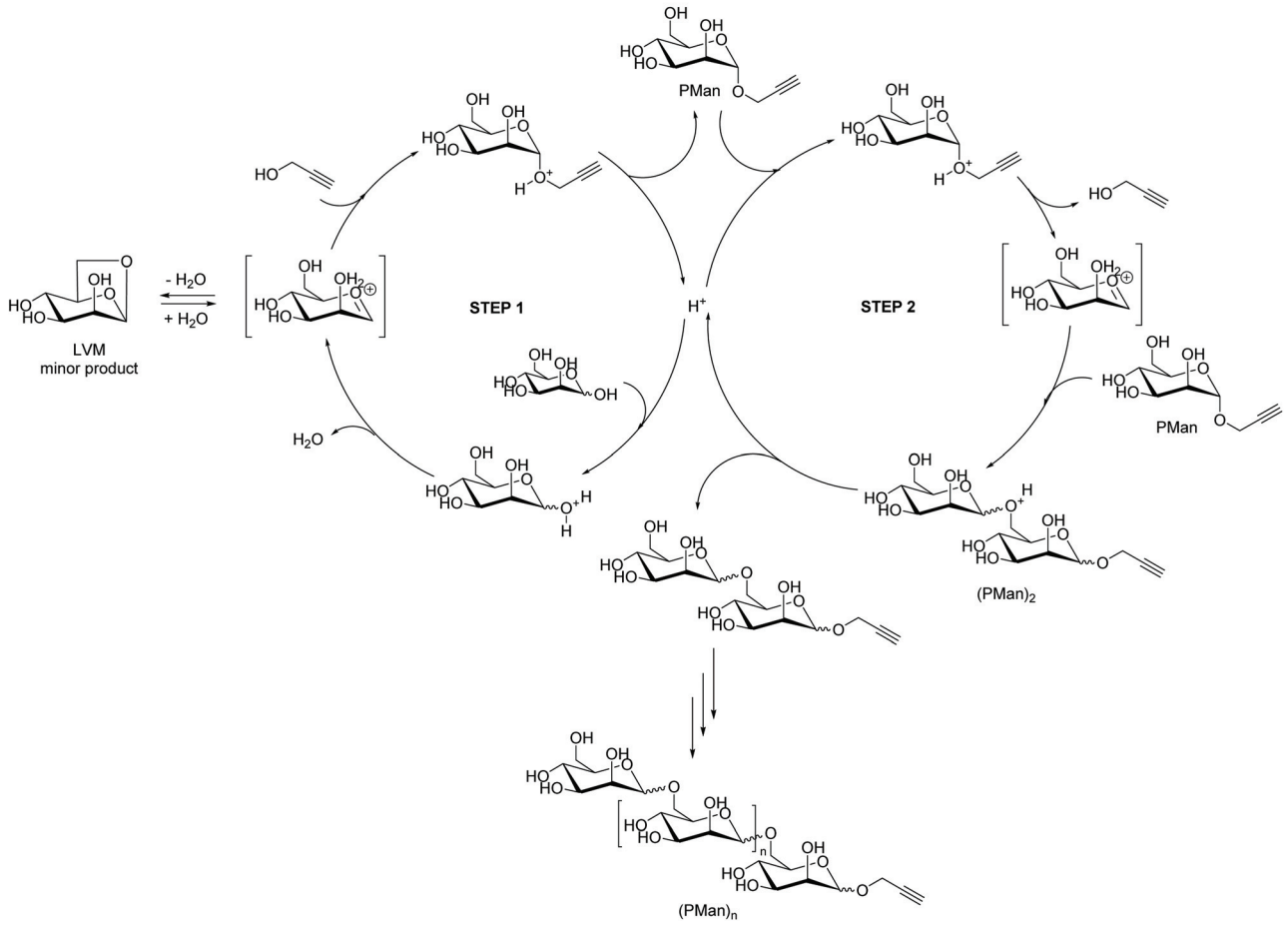

Scheme 2 Proposed reaction mechanism for step 1 and step 2.

Transposition to glucose

Finally, the reaction was transposed to glucose, which is even more attractive than mannose, as it is a product potentially derived from lignocellulosic biomass waste. The same conditions as those described above for steps 1 and 2 were applied. ^{1}H-NMR (Fig. S12†) spectroscopy and SEC analysis (Fig. S13†) confirmed the formation of propargyl-(oligo)-glucosides $(PGlu)_n$ with a $\overline{M_n}$ of 542 g mol^{-1} ($\overline{DP_n} = 3$) and a dispersity $Đ$ of 2.1. ^{1}H-NMR investigations clearly evidenced the presence of α- and β-anomers with the appearance of two signals for the alkyne protons (2.95–2.91 ppm) and two signals corresponding to the anomeric protons of the propargylated terminal position (α: 5.12 ppm, β: 4.67 ppm).

As stated in the Introduction section, the alkyne group at the chain-end of the prepared oligosaccharides (mannose and glucose) enables a direct access to amphiphiles. For this purpose, the well-known 'azide–alkyne Huisgen cycloaddition' presents an attractive method due to its atom-economy and quantitative conversions.[31] As demonstrated in previous studies,[5,32] this method is frequently utilized to prepare amphiphilic block copolymers and provides further applications of the as-prepared oligosaccharides. We show in a proof-of-concept experiment (Scheme 3) the successful addition of a long chain fatty acid (oleic acid) *via* click chemistry to mannose-oligomers (for more details, see

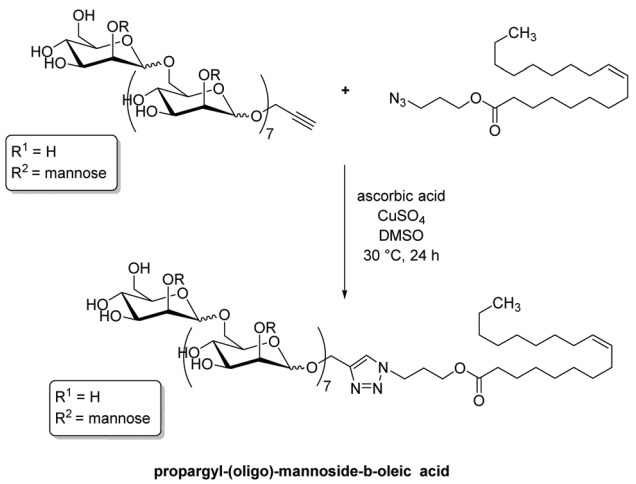

Scheme 3 Preparation of amphiphiles by the copper-catalyzed addition of oleic acid to $(PMan)_n$ *via* click-chemistry.

Fig. S14–S18†). The structure of the as-obtained amphiphile was evidenced by ^{1}H-NMR (Fig. S18†) with the appearance of the characteristic triazole peak at 8.1 ppm and the analysis by MALDI-TOF, which confirmed no depolymerization during the click reaction (Fig. S19†). This presents a powerful strategy to prepare amphiphilic APGs while avoiding the *in situ* depolymerization of oligosaccharides, as commonly observed with other functionalization methodologies.

Conclusions

In this work, we demonstrated that the acid catalyzed (amberlyst-15) glycosylation reaction of unprotected monosaccharides (mannose, glucose) and propargyl alcohol afforded fully functionalized propargylated glycosides with a $\overline{DP_n}$ up to 8 in 88% yield. The fine control of temperature, time and the molar ratio of sugar to alcohol could tune the $\overline{DP_n}$. Although the preparation of APGs with a $\overline{DP_n}$ more than 2 remains to date a huge challenge,[17,27–29] the proposed method could expand the molar mass and maintain the complete glycosylation of sugars at the same time. The distillation of water along with propargyl alcohol in step 2 proved to be the key step for the oligomerization. The elucidation of the structure by NMR spectroscopy strongly suggests that mannose-oligomers are mainly linked through α-(1,6)-glycosidic bonds, along with branching points at OH-2.

In a 'proof-of-concept' experiment, the alkyne function at the terminal end of the oligomers was exploited to add a long-chain fatty acid to the sugars *via* the Huisgen catalyzed 'Click-Chemistry'. We presented thereby an alternative method to synthesize oligosaccharide-based amphiphiles, which could be employed as bio-based surfactants. Further developments with respect to the synthesis of various oligosaccharide-based amphiphiles and investigations of their properties will be discussed in forthcoming contributions.

Conflicts of interest

There are no conflicts to declare.

Acknowledgements

The authors thank the CNRS, the Région Nouvelle Aquitaine, the University of Poitiers and the University of Bordeaux for their financial support. The authors are also grateful to the FR CNRS INCREASE for funding. CESAMO, Institut des Sciences Moléculaires (University of Bordeaux, Talence (33), France) is also acknowledged for MALDI-TOF MS experiments. Anne-Laure Wirotius is also strongly acknowledged for scientific discussion on NMR.

Notes and references

1 D. G. Hayes, D. K. Solaiman and R. D. Ashby, *Biobased Surfactants: Synthesis, Properties, and Applications*, Elsevier, 2019.
2 C. Stubenrauch, *Curr. Opin. Colloid Interface Sci.*, 2001, **6**, 160–170.
3 M. Henkel and R. Hausmann, in *Biobased Surfactants*, ed. D. G. Hayes, D. K. Y. Solaiman and R. D. Ashby, AOCS Press, 2nd edn, 2019, DOI: 10.1016/B978-0-12-812705-6.00002-2.
4 N. Albany, *Transparency Market Res.*, 2012, **82**, https://www.prnewswire.com/news-releases/specialty-surfactants-industry-is-expected-to-reach-usd-292-billion-globally-in-2017-transparency-market-research-161943735.html.
5 C. Schatz and S. Lecommandoux, *Macromol. Rapid Commun.*, 2010, **31**, 1664–1684.
6 S. de Medeiros Modolon, I. Otsuka, S. B. Fort, E. Minatti, R. Borsali and S. Halila, *Biomacromolecules*, 2012, **13**, 1129–1135.
7 I. Otsuka, K. Fuchise, S. Halila, S. Fort, K. Aissou, I. Pignot-Paintrand, Y. Chen, A. Narumi, T. Kakuchi and R. Borsali, *Langmuir*, 2010, **26**, 2325–2332.
8 J. Scheibel, *The impact of feedstocks on future innovation in surfactant technology for the detergent market: 98th American Oil Chemists Society Annual Meeting*, Quebec City, Canada, 2007.
9 C. Schatz, S. Louguet, J. F. Le Meins and S. Lecommandoux, *Angew. Chem., Int. Ed.*, 2009, **48**, 2572–2575.
10 https://www.gminsights.com/industry-analysis/biosurfactants-market-report.
11 J. Schulte, S. Enders and K. Quitzsch, *Colloid Polym. Sci.*, 1999, **277**, 827–836.
12 E.-M. Kutschmann, G. Findenegg, D. Nickel and W. Von Rybinski, *Colloid Polym. Sci.*, 1995, **273**, 565–571.
13 H. Luders, *Surfactant Sci. Ser.*, 2000, 77–84.
14 F. Jérôme, S. Marinkovic and B. Estrine, *ChemSusChem*, 2018, **11**, 1395–1409.
15 W. von Rybinski and K. Hill, *Angew. Chem., Int. Ed.*, 1998, **37**, 1328–1345.
16 K. Igarashi, in *Advances in Carbohydrate Chemistry and Biochemistry*, Elsevier, 1977, vol. 34, pp. 243–283.
17 K. Hill, W. Von Rybinski and G. Stoll, *Alkyl polyglycosides*, Wiley Online Library, 1997.
18 S.-I. Shoda, *Proc. Jpn. Acad., Ser. B*, 2017, **93**, 125–145.
19 R. M. Schmaltz, S. R. Hanson and C. H. Wong, *Chem. Rev.*, 2011, **111**, 4259–4307.
20 D. Svensson, S. Ulvenlund and P. Adlercreutz, *Biotechnol. Bioeng.*, 2009, **104**, 854–861.
21 M. S. U. Ackelid, presented in part at the Proc. Mat. Sci. Tech. Conf., Pittsburgh, PA, USA, 2009.
22 F. Orata, *Derivatization Reactions and Reagents for Gas Chromatography Analysis*, Masinde Muliro University of Science and Technology, IntechOpen, Kenya, 2012.

23 P. van der Peet, C. T. Gannon, I. Walker, Z. Dinev, M. Angelin, S. Tam, J. E. Ralton, M. J. McConville and S. J. Williams, *ChemBioChem*, 2006, **7**, 1384–1391.
24 A. L. M. Morotti, K. L. Lang, I. Carvalho, E. P. Schenkel and L. S. C. Bernardes, *Tetrahedron Lett.*, 2015, **56**, 303–307.
25 K. Bock and C. Pedersen, *J. Chem. Soc., Perkin Trans. 2*, 1974, 293–297, DOI: 10.1039/P29740000293.
26 P. Amaniampong, J.-L. Clément, D. Gigmes, C. Mellet, J. García Fernández, Y. Blériot, G. Chatel, K. Vigier and F. Jérôme, *ChemSusChem*, 2018, **11**(16), 2673–2676.
27 A. Karam, K. De Oliveira Vigier, S. Marinkovic, B. Estrine, C. Oldani and F. Jérôme, *ACS Catal.*, 2017, **7**, 2990–2997.
28 D. Geetha and R. Tyagi, *Tenside, Surfactants, Deterg.*, 2012, **49**, 417–427.
29 W. R. K. Hill, *Angew. Chem., Int. Ed.*, 1998, **37**, 1328–1345.
30 S. K. Mamidyala and M. Finn, *J. Org. Chem.*, 2009, **74**, 8417–8420.
31 V. K. Tiwari, B. B. Mishra, K. B. Mishra, N. Mishra, A. S. Singh and X. Chen, *Chem. Rev.*, 2016, **116**, 3086–3240.
32 J. Rosselgong, M. Chemin, C. C. Almada, G. Hemery, J. M. Guigner, G. Chollet, G. Labat, D. Da Silva Perez, F. Ham-Pichavant, E. Grau, S. Grelier, S. Lecommandoux and H. Cramail, *Biomacromolecules*, 2019, **20**(1), 118–129.